



## Reservoir Characteristics of a Quaternary Channel: Incorporating Rock Physics in Seismic and DC Resistivity Surveys

Jawwad Ahmad\*

University of Alberta, Edmonton, Alberta, Canada  
jahmad@phys.ualberta.ca

and

Douglas Schmitt

University of Alberta, Edmonton, Alberta, Canada

### Abstract

Buried channels are often filled with a variety of porous and permeable sediments which can act as water and hydrocarbon reservoirs. Shallow methane deposits within these channels (less than 50-m deep) represent a significant drilling hazard in some areas. We have earlier described the results of joint 10-km high resolution seismic reflection and DC resistivity profiles that were acquired in northwest Alberta to define the position, geological setting and reservoir characteristics of a buried channel. Interpretation of these along with well data reveals the presence of a channel and proves the purpose of study. At its deepest point, the channel cuts through more than 300-m of Cretaceous sands and shales and through a regional unconformity into higher velocity carbonates. The channel fill materials have generally lower seismic velocities and are more resistive than the flanking undisturbed Cretaceous formations. These contrasts allow the channel to be detected on the basis of both refraction and resistivity analysis. The resistivity profile further shows highly resistive zones that may be indicative of shallow gas which correspond to a known producing horizon. Physical and elastic properties of channel sand through geophysical logs were calculated using standard rock physics approach. Velocities of gas and water filled reservoir sand for different fluid scenarios were calculated using Gassmann's equation. Velocity – porosity and clay content trends were used to link sedimentological and rock physics properties into geological interpretation. High porosity and poorly consolidated channel sand shows variable seismic velocity that mainly depends on reservoir fluids. Log correlations were also established to see the lateral extent of facies.

### Introduction

In this article results of high resolution seismic and electrical resistivity tomography (ERT) surveys are discussed. Part of standard rock physics template as described in Avseth et. al., (2005), is used to interpret seismic data along with well log information. The details of seismic and ERT data acquisition are described in Ahmad et. al., (2005a and b). Where as interpretation of these data sets using conventional approach is described in Ahmad et. al., (2005c and d) and Pawlowicz et. al., (2005). Part of the processed seismic section overlaid with ERT profile is shown in Figure 1. The seismic data set is processed up to final stack using conventional processing flow with some

careful repetitive additional processing steps to enhance shallow reflections. The seismic section shows gas reservoir ~100 m. High resistivity values on ERT profile likely corresponds to gas at this depth. High amplitude reflections (bright spot) are also visible both on raw and processed data. Special attention was given to keep these high amplitude reflections during processing.

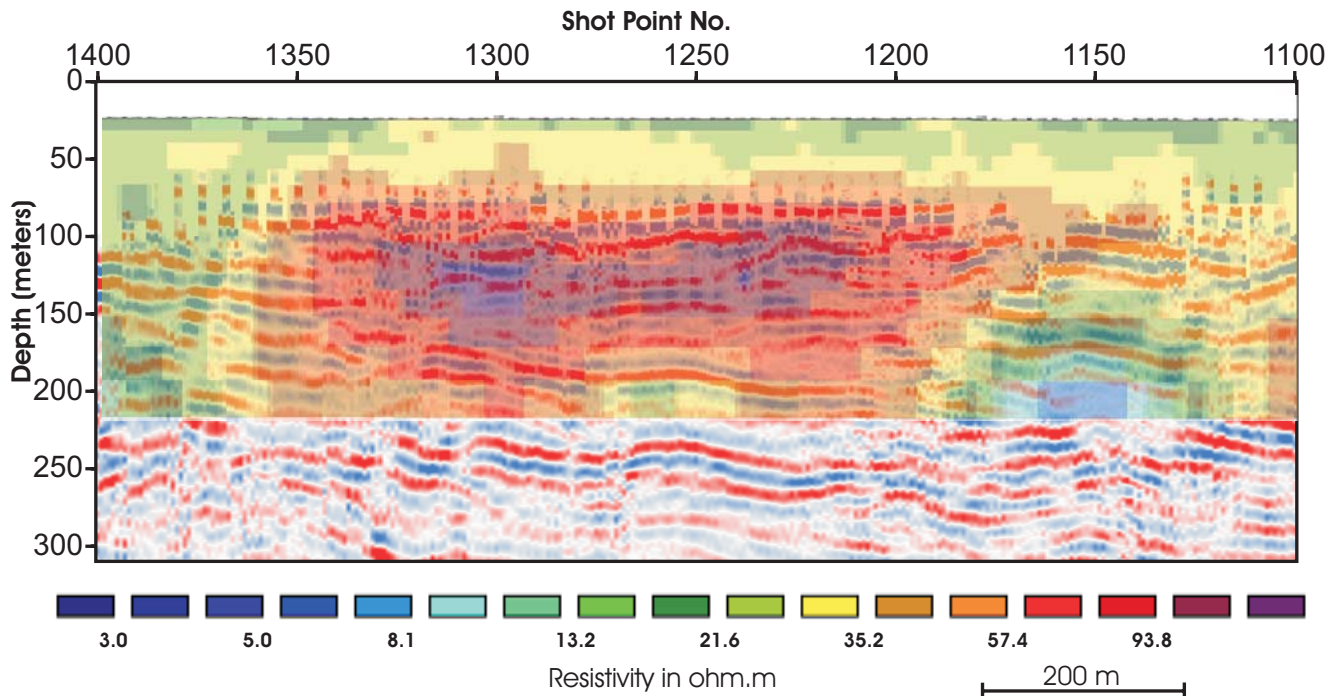


**Figure 1.** Part of the processed seismic section (30 fold) showing gas anomaly overlaid by electrical resistivity tomography (ERT) profile. Seismic section is depth converted using stacking velocities. ERT profile is after careful inversion. ERT is displayed using logarithmic color scale.

Unconsolidated Channel sand is at ultra shallow depth and possesses low seismic velocities. Well logs of few key wells are also used to define reservoir properties of channel sand. Not all wells have a sonic log at reservoir interval due to ultra shallow nature of gas reservoir. None of the well has a full waveform sonic log so only compressional sonic log was used. Elastic and physical properties are calculated using well logs. Gassmann's fluid substitution analysis is carried out to calculate affects of different fluids on compressional velocities ( $V_p$ ). The method for Gassmann's fluid substitution analysis was adapted from Smith et. al., (2003). Velocities are calculated using different fluid scenarios i.e., oil, water and gas. Gas properties required for input in Gassmann's equation are calculated using Batzal and Wang software package. Different gas properties are used in Gassmann's equation and finally gas properties at 1 MPa and 15 MPa are adapted for all calculations. Following is most commonly used form of Gassmann's equation:



$$K_{sat} = K^* + \frac{\left(1 - \frac{K^*}{K_0}\right)}{\frac{\phi}{K_{fl}} + \frac{(1-\phi)}{K_0} - \frac{K^*}{K_0^2}} \quad (1)$$

where  $K_{sat}$  = saturated bulk modulus,  $K_0$  = bulk modulus of the minerals,  $K_{fl}$  = bulk modulus of pore fluid,  $K^*$  = bulk modulus of porous rock frame, and  $\phi$  = porosity.

P wave velocity ( $V_p$ ) can be calculated once ' $K_{sat}$ ' is calculated for desired fluid saturation using Gassmann's equation.

$$V_p = \sqrt{\frac{K_{sat} + \frac{4}{3}G}{\rho_B}} \quad (2)$$

Where  $G$  = shear modulus;  $\rho_B$  = bulk density;  $K_{sat}$  = saturated bulk modulus

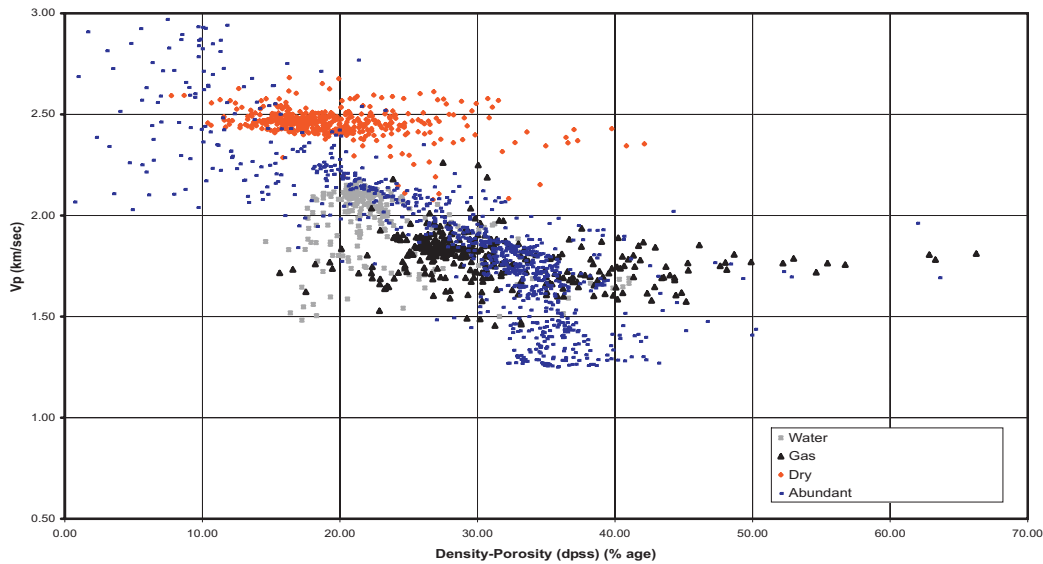
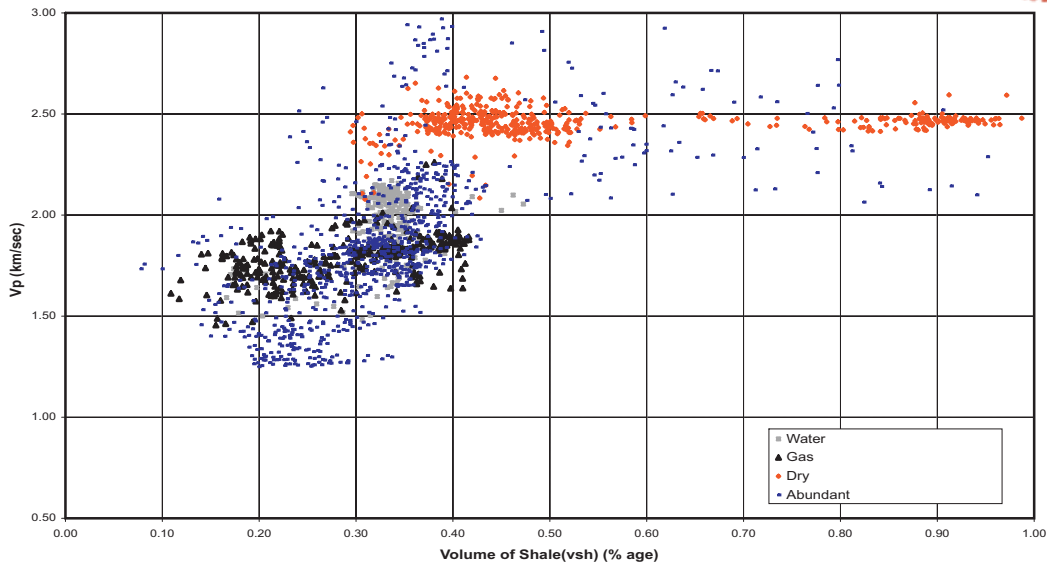


**Figure 2. (a)  $V_p$  vs Porosity plot of four different wells.  $V_p$  is decreasing as porosity is increasing which is in agreement with the results of laboratory measurements presented by Han et. al., (1986)**



(b)

**Figure 2. b) Vp vs volume of shale plot of four wells. Gas bearing well shows low Vp as compared to water bearing well.**

### Effects of porosity and clay content on Vp and frame properties

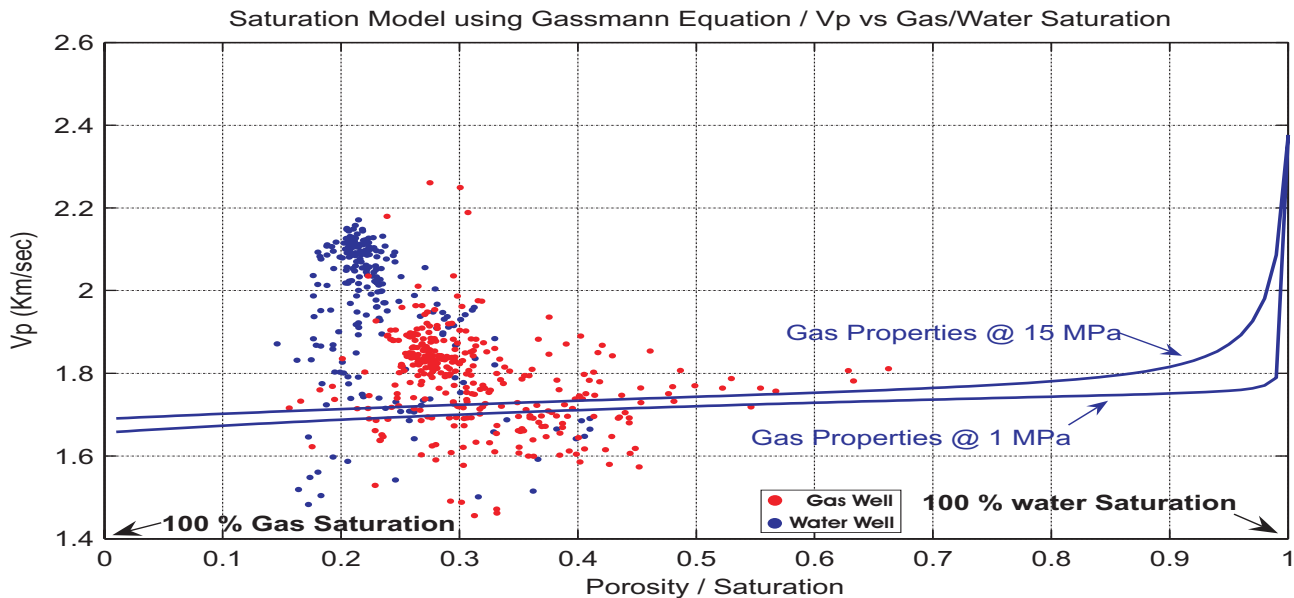
In consolidated sandstones the porosity tends to decrease with the increase in Vp. As porosity and clay content are interrelated it is true that Vp decreases with increase in clay content, but this is not always true. Steeper trends in velocity porosity cross plot are due to diagenesis and cementation effects. Whereas, data from one reservoir or narrow depth range shows flatter trend, also known as deposition trends which is the case here in channel sand. Usually young unconsolidated sands have Vp ~2 km/sec or slightly less than this (see figure 1 & 2 of Bachrach and Nur, (1998) for ultra low velocity (<300 m/sec) of beach sand and Gassmann's fluid substitution effects). The channel sandstone under investigation is grain supported fine-grained unconsolidated sandstone. Variations in the pore shape also effect velocity-porosity trends. Different sand models for calculating bulk modulus of rock matrix ( $K_{matrix}$ ) are described by Mavko et. al., (1998) and one of the model 'Marion-Yin Model' affectively applied to calculate physical properties of the stratigraphic sequence (Florez et. al., 2003) keeping the consideration of deposition, compaction and cementation trends. Careful experimental analysis for frame properties on quartz sandstone by Murphy et. al., (1993) showed that both bulk and shear moduli depend on porosity but the ratio of Vp/Vs is independent of the porosity.

Figure 2a shows P wave velocity (Vp) vs porosity cross plot of few Quaternary wells at reservoir interval. Vp is decreasing as porosity is increasing, which is in agreement with the results of a laboratory measurements presented by Han et. al., (1986). Volume of clay in the sandstone lowers the effective bulk modulus ( $K_{eff}$ ) and ultimately P wave velocity (Han et. al., 1986). But this case is not always true; Figure 2b shows Vp vs Volume of clay cross plot and it is clear that at least in one well Vp is increasing with the increase of clay content.

### Elastic Properties of Channel Sand

Bulk modulus of mineral matrix ( $K_{\text{matrix}}$ ) along with Voigt-Reuss-Hill (VRH) and Hashin-Shtrikman (HS) bounds are calculated for analysis. Bulk modulus of mineral matrix ( $K_{\text{matrix}}$ ) has range form 13 to 23 GPa which is within the bounds calculated for sand i.e., quartz and clay mixture (see figure 4 of Han and Batzle, (2004) for upper and lower bounds of different sandstones from published case studies).  $V_p$  calculated after substituting gas and water in desired depth interval using Gassmann's equation is displayed in Figure 3.  $V_p$  calculated after gas substitution is lower than water, which is according to the prediction of Gassmann's theory.

Elastic moduli i.e.,  $K^*$  (dry rock with in-situ fluid),  $K_{\text{matrix}}$ ,  $K_{\text{eff(water)}}$ , and  $K_{\text{eff(gas)}}$ , for one key Quaternary well are shown in Figure 4. Elastic properties are variable for each type of sandstone i.e., consolidated or unconsolidated etc. Effective bulk modulus of reservoir part of one Quaternary type well is shown in Figure 4a (for sand classification with reference to bulk modulus see fig. 2.7 of Avseth, 2000). Figure 4b shows the  $K_{\text{eff}}$  for in-situ fluid filled, dry, gas saturated and water saturated unconsolidated channel sandstone. The unconsolidated reservoir sand shows fairly low velocity ( $\sim 1.8$  km/sec) which is due to the less depth of burial and geological age i.e., Quaternary (see table-4 of Avseth, 2000 for sand facies classification based on elastic properties). Diagenetic and sedimentological trends also alter  $V_p$  and can be correlated and used for velocity prediction away from well location and add to the seismic interpretation (Avseth et. al., 2005).



**Figure 3. Saturation model using Gassmann's equation. Bottom curve is fluid substitution using density and bulk modulus of gas at 1MPa @ 16°C and top curve at 16 MPa. These are best estimates for gas properties because of Ultra shallow nature of reservoir.**

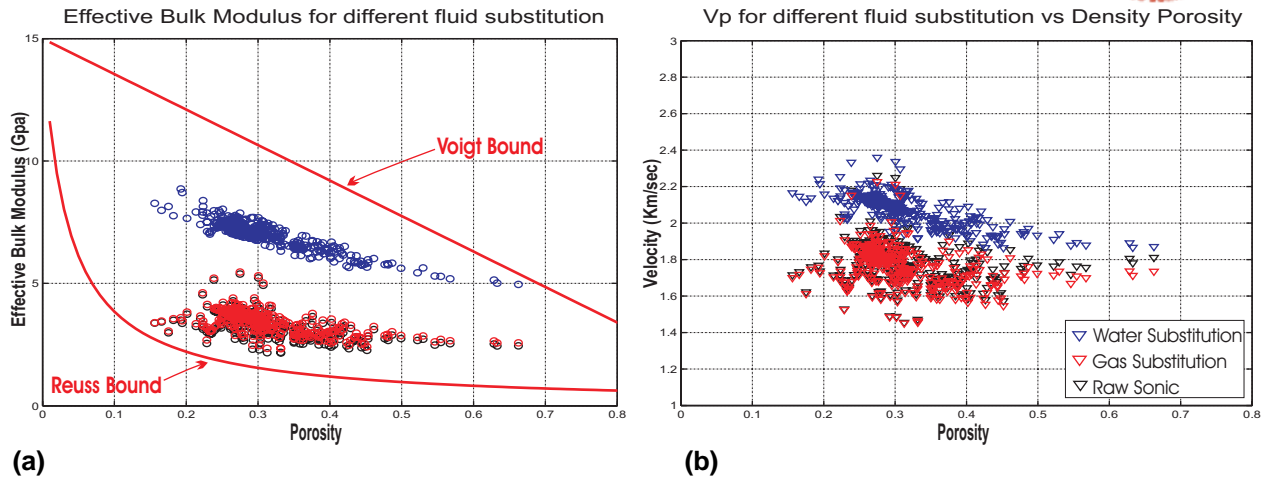


**Figure 4. Fluid substitution effects on Vp and Effective bulk modulus for one Quaternary well. (a) Effective bulk modulus as a function of porosity; raw bulk modulus (black); after water saturation (blue); and after gas saturation (red). Voigt-Reuss bounds are also shown here. (b) Original Vp based on sonic log (black); Vp after water saturation (blue); and Vp after gas saturation (red).**

### Case Study

Fluid substitution using Gassmann's equation was carried out on ultra shallow Quaternary wells of northwest Alberta and corresponding velocities were calculated (result of one representative well is shown here). Geological description of sand encountered in nearby well is as follows: 'sandstone white-light grey translucent very fine grained subrounded-subangular grains, loose unconsolidated'.

The available geophysical logs for Quaternary wells are: gamma ray; density-porosity; sonic (compressional wave only); deep, medium and shallow resistivity; neutron-porosity. Volume of shale log available with geophysical logs was not appropriate to use for shallow part of the well. It shows very high shale content probably due to the high gamma ray value somewhere in deeper part of the well, which is due to the presence of high radioactivity shale in that area. After careful analysis of gamma ray logs and literature review, volume of shale was calculated based on gamma ray log using sand line at 30 gAPI and shale line at 200 gAPI. Water saturation was not available for all wells and density-porosity was used instead. It is also practice to use neutron-porosity, but it is not recommended because it did not give reliable results in case of hydrocarbons (Avseth, et. al., 2005).

### Quaternary Well # 1 (Gas)

Figure 5 shows the logs of Quaternary well with depth interval from 60 to 75 meter. The measured data consists of gamma ray/volume of shale on track-1, density/sonic on track-2, shallow/medium/deep resistivity on track-3, neutron/density porosity on track-4, Bulk modulus/shear modulus of mineral and bulk modulus of dry matrix on track-5, and velocities calculated after Gassmann's fluid substitutions (gas/oil/water) on track-6. Gassmann's fluid substitution was carried out using two different gas properties. Gas properties calculated at 1 MPa and 15 MPa at temperature 16 °C using Batzal's software package. Gas reservoir encountered in this well was from 64 to 73 meter with two separate pockets (see resistivity log on track-3, Figure 5). As the gas reservoir is very shallow and at low pressure (reservoir pressure ~ 600 KPa)



approximation of using 1Mpa for gas properties calculation is appropriate. Water saturation log was not available for input in the Gassmann's fluid substitution analysis so, saturation was assumed from density-porosity log. A hybrid approach can also be applied to extract water saturation from resistivity log combined with density-porosity and/or neutron-porosity logs as described in Avseth, (2000).

### Conclusion

The Gassmann's fluid substitution analysis was carried out on real data and frame properties and fluid effects on wave velocities for one selected Quaternary well with ultra shallow Channel sand reservoir is tested. Effective bulk modulus for gas and water is calculated for channel sand that is used to calculate compressional wave velocities. Effective bulk modulus after substituting water in Gassmann's equation gives higher values as compared to gas substitution. Channel sand is unconsolidated and shows slightly lower compressional wave velocity (~1.8 km/sec). Compressional wave velocity and porosity cross plot was developed that shows decrease of velocity with increase of porosity for slightly deeper well and relatively flat trend for other shallower well. Velocity and volume of shale cross plot shows variable trends for shallow wells.

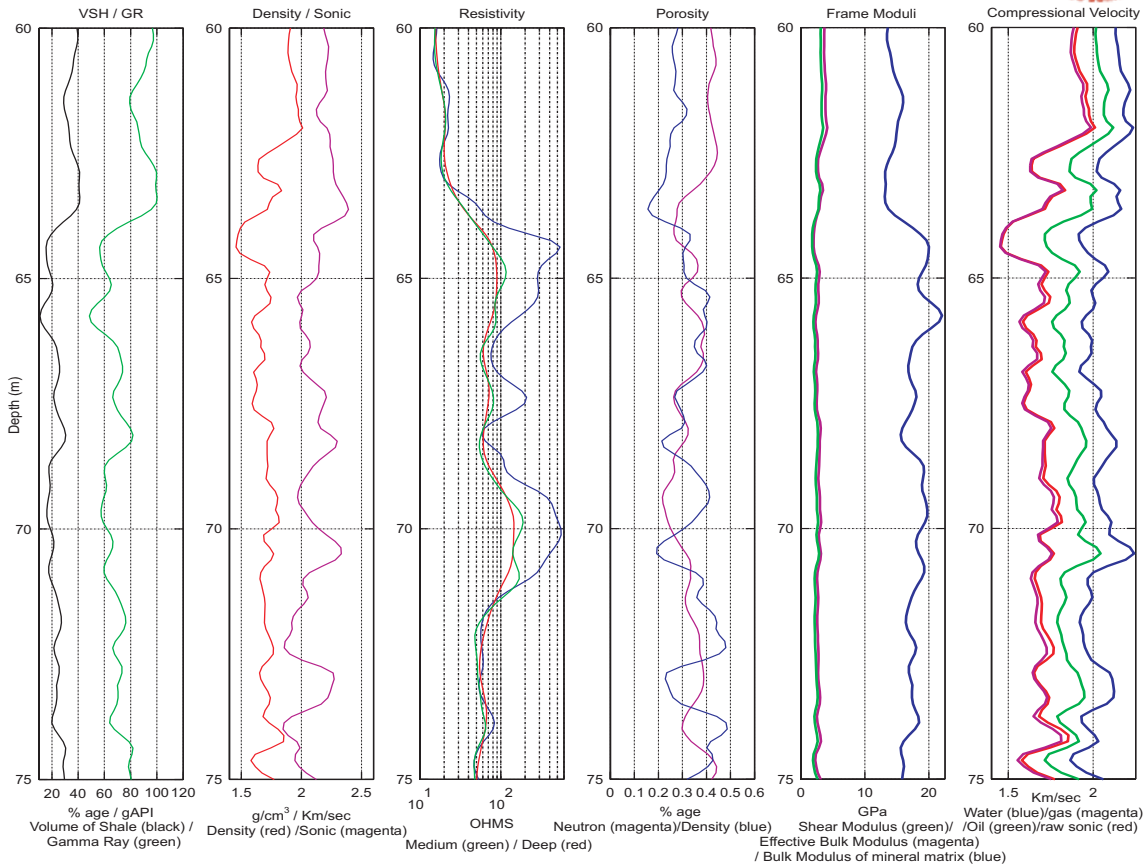


Figure 5. Fluid substitution result of gas bearing well. From left to right panels numbers are in increasing order. 1<sup>st</sup> panel gamma ray log and volume of shale log calculated from gamma ray log. 2<sup>nd</sup> panel density and sonic log. 3<sup>rd</sup> panel resistivity log showing high resistivity and corresponding hydrocarbon bearing zone at 63 meter. 4<sup>th</sup> panel density-porosity and neutron porosity. 5<sup>th</sup> panel showing bulk modulus  $K^*$  and shear modulus  $G$  for mineral matrix; both has very less separation which shows more sand and less shale. Blue curve is bulk modulus for mineral matrix. 6<sup>th</sup> and last panel shows original sonic ( $V_p$ ) velocity and calculated velocities ( $V_p$ ) with different fluid substations using Gassmann's equation. Sonic raw velocity (red); Gas substitution (magenta); oil substitution (green); and water substitution (blue).  $V_p$  with gas substitution is very close to the recorded sonic velocity. Density-porosity is used for fluid substitution.



## References

- Ahmad, Jawwad, Douglas R. Schmitt, Dean Rokosh, John G. Pawlowicz, Mark M. Fenton, and Alain Plouffe, 2005(a), Seismic imaging of Quaternary channels, Rainbow Lake, Northern Alberta, Canada: Expanded Abstract, Presented at CSEG Annual Convention 2005, Calgary
- Ahmad, Jawwad, Douglas R. Schmitt, Dean Rokosh, John G. Pawlowicz, and Alain Plouffe, 2005(b), Seismic imaging of Quaternary channels, Rainbow Lake, Northern Alberta, Canada: Expanded Abstract, Presented at AAPG Annual Convention 2005, Calgary
- Ahmad, Jawwad, and Douglas R. Schmitt, 2005(c), Seismic and resistivity imaging for Quaternary Channels: Rainbow lake, Northwest Alberta, Canada, CSEG Recorder, 30 (9), 40-43
- Ahmad, Jawwad, Douglas R. Schmitt, Dean Rokosh, John G. Pawlowicz, and Alain Plouffe, 2005(d), Seismic and DC resistivity imaging of a buried channel, NW Alberta, Canada, Poster Presentation at AGU Annual Meeting, 2005, San Francisco.
- Avseth Per, Tapan Mukerji, and Gary Mavko, 2005, Quantitative Seismic Interpretation: Applying rock physics tools to reduce interpretation risk: Cambridge University Press
- Avseth, Per, 2000, Combining rock physics and sedimentology for seismic reservoir characterization of North Sea turbidite systems: Unpublished Ph.D. thesis, Stanford University.
- Bachrrach Ran, and Amos Nur, 1998, High-resolution shallow-seismic experiments in sand, Part 1: Water table, fluid flow, and saturation, Geophysics, **63**, 1225-1233
- Florez Juan, and Gary Mavko, 2003, Porosity-Velocity distribution in stratigraphic sequences: The Marion-Yin Model: Search and Discovery article#40105, expanded abstract AAPG annual meeting 2003
- Han, De-hua, and Michael L. Batzle, 2004, Gassmann's equation and fluid-saturation effects on seismic velocities: Geophysics, **69**, 398-405
- Han De-hua A, Nur, and Dale Morgan, 1986, Effects of porosity and clay contents on wave velocities in sandstone: Geophysics, **51**, 2093-2107
- Mavko, Gary, Tapan Mukerji, and Jack Dvorkin, 1998, The rock physics handbook: Tools for seismic analysis in porous media: Cambridge University press
- Murphy William, Andrew Reischer, and Kai Hsu, 1993, Modulus decomposition of compressional and shear velocities in sand bodies: Geophysics, **58**, 227-239
- Pawlowicz, G. John, Tami J. Nicoll, Mark M. Fenton, Jawwad Ahmad, Douglas R. Schmitt, Dean Rokosh, and Alain Plouffe, 2005, Paleovalleys Revealed by Bedrock Topography and Drift thickness Mapping Show Potential for Shallow Gas, Northwestern Alberta, Canada: Search and Discovery Article #10086 (2005)
- Smith, M. Tad, Carl H. Sondergeld, and Chandra S. Rai, 2003, Gassmann fluid substitutions: A tutorial: Geophysics, **68**, 430-440